# Fluid imbibition in paper fibers: Precursor front

Eduardo N. de Azevedo,[1] Lars R. Alme,[2,*] M. Engelsberg,[3,†] Jon Otto Fossum,[2] and Paul Dommersnes[4]
[1]*Programa de Pós-Graduação em Ciência de Materiais, Universidade Federal de Pernambuco, Cidade Universitária, 50.670-901, Recife, Pernambuco, Brazil*
[2]*Department of Physics, Norwegian University of Science and Technology, Hoegskoleringen 5, NO-7491, Trondheim, Norway*
[3]*Departamento de Física, Universidade Federal de Pernambuco, Cidade Universitária, 506701-901, Recife, Pernambuco, Brazil*
[4]*Laboratoire Matière et Systemes Complexes, Université Paris Diderot-Paris 7, Bâtiment Condorcet, 10 rue Alice Domon et Lónie Diuquet, 75205 Paris Cedex 13, France*
(Received 29 August 2008; published 31 December 2008)

We employ nuclear magnetic resonance imaging to study water penetration in cylindrical blocks of unsized paper prepared under different molding pressures. From the measured kinetics of the imbibition profiles, we determine the dependence of the effective transport diffusivity upon degree of saturation of the pores by the penetrating fluid. In general, the transport process is found to be non-Fickian and we discuss different methods of data analysis adapted to this situation. The effective transport diffusivity vividly captures the presence of a precursor front, consisting of fluid in partially filled pores, with a much higher effective diffusivity than that of fluid in largely saturated pores.

DOI: 10.1103/PhysRevE.78.066317 PACS number(s): 47.56.+r, 76.60.Pc, 47.55.nb

## I. INTRODUCTION

Fluid penetration in porous systems has been extensively studied given its relevance to many important processes. It has long been known that the generalization to real porous systems of the pioneering work of Washburn [1] on fluid transport in capillaries is not straightforward. It has been found, for example, for some types of real pore structures, that the distance traveled by the fluid in a given time interval cannot be assumed to be simply proportional to the diameter of the pores [2]. Paper fibers are another example where continuous displacement of a meniscus along bulk pores, as in Washburn's model, has been found to be a rather inefficient process [3]. The particular pore morphology of paper, where overlapping fibers form a highly interconnected network of flow paths, appears to favor a film flow along channels formed by fiber overlap [3]. It has been argued that the displacement of a meniscus along bulk pores in paper should be strongly hindered by the presence of discontinuities at the pore junctions.

Fluid imbibition in porous systems has been studied by a variety of techniques. In some systems, such as paper fibers, the process could be visualized at the microscopic level using cryoscanning electron microscopy (cryo-SEM) [3]. This permitted the observation of transport paths along the actual pores and channels. On the other hand, imaging techniques, for example, magnetic resonance imaging, can yield moisture profiles coarse-grained over the dimension of a voxel, typically a cube of 1 mm on each edge, which includes a large number of pores. In this work we demonstrate that this coarse-grained approach, in the case of paper fibers, yields results, which are consistent with the microscopic observations.

In many cases involving rigid, or consolidated porous systems, with no interaction between the fluid and the solid matrix, Fickian behavior appears to prevail with transport diffusivities, which are usually strongly dependent upon fluid concentration [4–8]. Under these conditions the moisture dependence of the transport diffusivity can be determined from measured MRI moisture profiles, and a correlation with microscopic process can be attempted. On the other hand, for nonconsolidated porous systems, such as our unsized paper cylindrical blocks, fluid intake can modify the permeability which may become time dependent. Chemical effects involving the fluid and the matrix can also take place further modifying pore morphology, especially when the fluid is water. Moreover, the transport process involves not only a liquid and a solid phase but also a vapor phase, which condenses in some regions while liquid water evaporates in other regions. In all these cases, departures from Fickian behavior could be expected and have been reported [9–12].

The most frequent departure from the Fickian regime in porous systems entails subdiffusive behavior whereby fluid transport, for long times, is delayed compared to normal Fickian diffusion. In this paper we will discuss different strategies that have been adopted by various authors to accommodate departures from Fickian behavior into a formalism where the starting assumption is Darcy's law. The aim is to determine a moisture-dependent transport diffusivity and to correlate it with the morphology of paper pores and with microscopic observations in paper fibers.

## II. EXPERIMENTAL DETAILS

Magnetic resonance imaging (MRI) experiments were performed at 85 MHz using a Varian Inova spectrometer, which includes a 2-T, 30-cm bore superconducting magnet [11]. The sample was a solid cylinder typically 2.2 cm in diameter with a length of 11.4 cm contained in a plastic tube made of PVC, oriented with its cylindrical axis along the horizontal direction. One end of the sample was placed in

*Present address: Det Norske Veritas, Ingvald Ystgaards vei 15, N-7496, Trondheim, Norway.
†Author to whom correspondence should be addressed; mario@df.ufpe.br

 

contact with a water reservoir consisting of an L-shaped PVC tube attached to the sample tube by a threaded coupling. At $t=0$ the L-shaped tube was filled with water and the level was maintained with negligible over-pressure. A plastic grid separated the water reservoir from the sample.

The starting material for the preparation of these cylinders was grade 1 filter paper, manufactured by Whatman Int. Ltd., containing at least 98% of, largely water-insoluble, pure alpha cellulose. The thin circular disks were first cut into rectangular strips and placed in a regular paper shredder where they were reduced to thin strips approximately 1.5-cm long by 2-mm wide. In a second stage of partitioning these thin strips were placed in a grinding machine and cut, with its fast rotating blade, for approximately 30 s. The resulting material, when observed through a microscope, appeared as an entanglement of mostly individual cellulose fibers where all directionality had been lost.

A cylindrical PVC tube, externally reinforced by a brass cylinder, was filled with these cellulose fibers and pressures of up to 30 MPa were applied using a manual hydraulic press. No noticeable expansion was noticed after the pressure was released. Most of the data reported here correspond to a solid cylinder compressed by an applied pressure of 27.5 MPa, although some reference will also be made to a cylinder compressed by an applied pressure of 13.6 MPa. For this range of molding pressures (10–30 MPa) the resulting material appeared to be relatively uniform from the point of view of MRI. Although inhomogeneities in the permeability induced by the compression process still caused some observable effect in the images, the fluctuations could be considered tolerable. Furthermore, the average permeability to water imbibition was sufficiently reduced in this molding pressure range to permit measurements with acceptable time resolution.

A three-dimensional (3D) gradient spin-echo sequence with echo time $TE=1.1$ ms and repetition time $TR=300$ ms was employed with an acquisition matrix of size $128\times32\times32$, with 32 steps in each phase encoding gradient [13]. Each point in a moisture profile, corresponding to a given time after the beginning of imbibition, consisted of the average signal amplitude in one of the 128, approximately 1 mm thick, successive disks along the cylindrical axis of the sample. Each disk was defined by a matrix of $32\times32$ pixels whose average signal amplitude represents a single point in the profile. By this procedure any information about possible kinetic roughening effects on the imbibition fronts [14] is, in principle, lost. However, images of longitudinal slices of the cylinder as a function of time did exhibit some roughening, which was found to be more pronounced in the slower moving front than in the faster one. Unfortunately signal intensity variations caused by inhomogeneities produced in the sample preparation process and the relatively poor resolution of only 32 pixels prevented a quantitative study of the kinetic roughening effect in our samples.

The total acquisition time for each image, from which a moisture profile was extracted, was approximately 5 min and the imbibition time, in the data quoted below, was defined using the center of acquisition interval.

The spin-lattice relaxation was artificially shortened to achieve better time resolution. To that end a small amount of $CuSO_4$ was added to the water in the reservoir bringing down its spin-lattice relaxation time to $T_1\approx115$ ms.

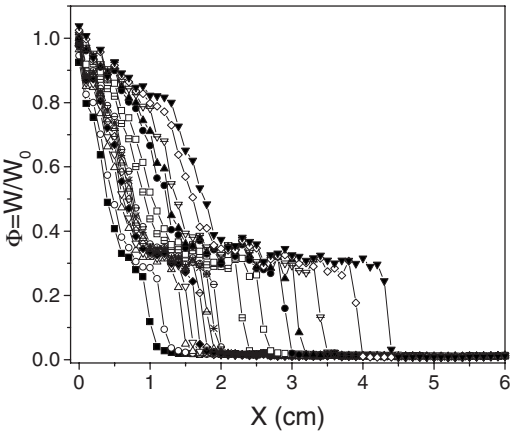


FIG. 1. Moisture profiles in a pressure-molded (27.5 MPa) paper cylinder as a function of time after the beginning of imbibition. Imbibition times range from (■) 11 to (▼) 434 min with intermediate values $t=16$, 27, 32, 37, 42, 48, 53, 58, 89, 120, 152, 178, 218, and 359 min. The solid lines are an aid to the eye.

## III. RESULTS AND DISCUSSION

The moisture profiles shown in Fig. 1 correspond to times of imbibition ranging from 11 to 434 min. The uncertainty in the value of $\Phi$ arising from finite signal-to-noise ratio is represented approximately by the size of the symbols in Fig. 1. However, some larger fluctuations, such as at $x=2.7$ cm and $x=0.3$ cm, are also apparent and can be attributed to inhomogeneities resulting from the sample preparation process.

The profiles of Fig. 1 and also those obtained using cylindrical blocks subjected to different molding pressures, show a common aspect. Qualitatively, all profiles exhibit a characteristic feature consisting of a fast moving precursor front, corresponding to regions where the moisture content is well below saturation ($\Phi=W/W_0\approx0.31$), and a slower moving front in regions where the pores are close to saturation ($\Phi=W/W_0\approx1$). Here $W_0$ denotes the saturation concentration. It is worth pointing out that the precursor front observed in Fig. 1 has a flat profile with a quite well-defined value of $\Phi$ and is therefore qualitatively different from the one discussed earlier by Bico and Quéré [2].

Although in MRI each point in the moisture profile is coarse grained over a large number of pores and channels, these two characteristic fronts will be shown to be consistent with results of cryo-SEM [3] in unsized paper sheets.

Attempting to understand, from fluid mechanics arguments, two-phase liquid flow in such an enormously complex network of interconnecting pores as paper is quite challenging. On the other hand, compared to other porous systems, paper exhibits some characteristic feature that may lead to an experimentally observable signature of a particular transport process.

Paper is composed of cellulose fibers with lengths in the millimeter range and quite uniform cross-sectional dimen-

sions [3] (~15-$\mu$m width and 5–10-$\mu$m thickness). This relatively well-defined characteristic cross section leads to a rather sharp separation between film flow and flow along the bulk of the pore space. Given the high degree of overlap of cellulose fibers many small channels are created along fiber overlap regions. Such fiber overlap channels open up to significantly larger bulk pores as one moves away from the fibers. Furthermore, the bulk pores are highly interconnected and may have enormously variable cross sections, but the small channels formed by fiber overlap are believed to have relatively uniform dimensions. Typically, the depth of a channel from its bottom to the channel-pore interface has been found to be [3] 1–3 $\mu$m in unsized paper sheets.

The classical type of flow, first described by Lucas [15] and Washburn [1], whereby the fluid meniscus continuously advances inside a capillary is believed to be much more complex in a network of highly interconnected pores, especially when several pores meet at a junction. It has been suggested that only when the majority of pores at a junction are filled with wetting fluid can the meniscus continue to penetrate frontally. Otherwise, it will remain stationary when the junction is reached and further advance can only take place by film flow along the highly interconnected network of small channels formed by fiber overlap [3]. Because of the enormously large number of bulk pore junctions, and the large probability of stationary points in classical piston-type flow, film flow can be expected, and has actually been found to constitute the predominant transport process in unsized paper sheets [3]. As a consequence of this discussion, the faster imbibition front of Fig. 1 could be considered a signature of film flow taking place in regions where the bulk pores are far from being saturated by the wetting fluid.

A different level of description of fluid imbibition, which does not require a detailed fluid mechanical calculation, and is more suitable from the point of view of a coarse-grained approach, has been also employed. The starting point is Darcys law: $J=-K\partial P_c/\partial x$ [for a one-dimensional (1D) case], where $J$ denotes the local volumetric flux and $K=\kappa/\mu$, is the ratio between the permeability $\kappa$ of the medium and the viscosity $\mu$ of the fluid. The term macroscopic capillary pressure is usually employed for the quantity $P_C$. It is defined as the difference between the pressures of the water phase and the air phase averaged over a small, but macroscopic, representative elementary volume containing many pores. If $P_c$ and $K$ are assumed to be functions of moisture content $\Phi=W/W_0$ only, one can further write $J=-K(\Phi)(\partial P_c/\partial\Phi)(\partial\Phi/\partial x)$. Moreover, by combining Darcy's law with the continuity equation one obtains

$$\frac{\partial\Phi}{\partial t}=\frac{\partial}{\partial x}\left(D(\Phi)\frac{\partial\Phi}{\partial x}\right). \tag{1}$$

In Eq. (1) $D(\Phi)$ is the transport diffusivity given by $D(\Phi)=K(\Phi)\partial P_c/\partial\Phi$, which, in this approach, is expected to contain all the information necessary to characterize the imbibition process in the porous system.

If the imbibition experimental conditions can be approximately represented by a water reservoir at $x<0$ in contact with a semi-infinite porous system at $x\geqslant 0$, one can take advantage of Boltzmann transformation [16] of the 1D diffusion equation. This is achieved by introducing a new variable $\eta=x/t^{1/2}$, which transforms Eq. (1) into an ordinary differential equation in the single variable $\eta$. Since not only Eq. (1) but also the boundary conditions, $\Phi(\eta=0)=1$, $\Phi(\eta\rightarrow\infty)=0$, can be represented in terms of the variable $\eta$ alone, it follows that the moisture content must also be a function of $\eta$ only. Hence, if measured moisture profiles at different times are plotted as a function of the variable $\eta=x/t^{1/2}$ they should collapse into a universal curve. Furthermore, the moisture-dependent transport diffusivity $D(\Phi)$ can be extracted from this universal curve $\Phi(\eta)$ [16],

$$D(\Phi)=-(1/2)\left(\frac{d\eta}{d\Phi}\right)\int_0^\Phi \eta(\Phi')d\Phi'. \tag{2}$$

It has been found experimentally in many cases [4–8], especially when water imbibition in construction materials is involved, that a universal curve $\Phi(\eta)$ is actually obtained when moisture profiles are plotted as a function of the variable $\eta=x/t^{1/2}$. Moreover, using Eq. (2), moisture-dependent transport diffusivities have been determined [6,7], although it has seldom been possible to achieve a clear correlation between $D(\Phi)$ and the morphology of the porous system. It will be shown that, in the present system, such a correlation is possible.

Some difficulties may arise when one tries to apply Eq. (2) to experimental data. In some cases it is found that moisture profiles do not really collapse into a universal curve when plotted as a function of $x/t^{1/2}$. This is perhaps not too surprising since some of the assumptions leading to Eq. (1) may not be satisfied. It has been pointed out, for example [17,5], that the penetrating fluid may interact with the solid matrix causing changes in the pore morphology and that the permeability and transport diffusivity may become explicitly time dependent.

Another possible source of so-called non-Fickian behavior arises from the fact that the imbibition process involves not only wetting fluid transport but also vapor transport. If vapor and fluid can be considered to reach immediate equilibrium, Eq. (1) is still applicable to the fluid concentration $\Phi$. However, if there is a time dependence associated with the phase change between fluid and vapor, the transport of each phase must be modeled separately [10]. Two coupled Fickian equations, one for each phase, are then needed and a continuity equation cannot be assumed to hold for the fluid phase alone, as done in Eq. (1).

There have been a few attempts, which, although still following the basic steps of Eqs. (1) and (2), enable one to deal with non-Fickian behavior. One of these approaches assumes an explicit, separable, time dependence in the transport diffusivity $D(\Phi,t)=\gamma(t)\delta(\Phi)$ of Eq. (1). This can be easily shown, assuming the same boundary conditions as for Eq. (1), to also lead [9] to a universal curve provided the moisture profiles are plotted as a function of the new variable $\xi=x/\tau^{1/2}$, where $\tau=\int_0^t\gamma(t')dt'$. In Fig. 2 the measured profiles of Fig. 1 are plotted as a function $x/t^{1/2}$. The results suggest that the data fail to collapse into a universal curve, as expected from Fickian behavior. However, if the measured profiles are instead plotted as a function of $x/t^{0.40}$, as shown in

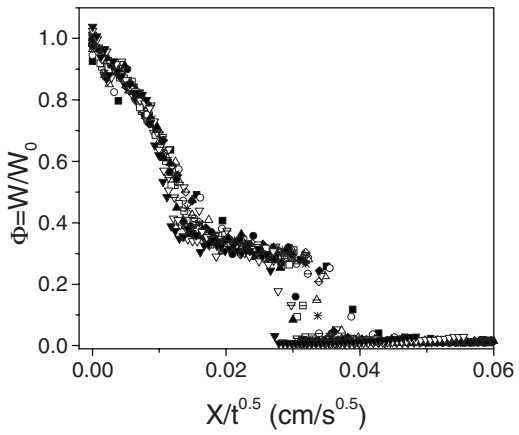


FIG. 2. Moisture profiles of Fig. 1 plotted as a function of $x/\sqrt{t}$. Symbols denoting different times are the same used in Fig. 1.

Fig. 3, the data appear to collapse into a universal curve to a reasonably good approximation. It is worth pointing out that the value $0.40 \pm 0.02$ of the exponent is not, by any means, universal and may change drastically if the sample preparation conditions are altered. For example, for a paper sample prepared under a molding pressure of 13.6 MPa we found the exponent to be close to 0.24.

We next assume a separable time-dependent transport diffusivity of form $D(\Phi,t)=\gamma(t)\delta(\Phi)$ with $\gamma(t)=0.8t^{-0.20}$ and define the variable $\xi=x/\tau^{1/2}$, where $\tau=\int_0^t \gamma(t')dt'=t^{0.80}$. Thus, the choice of a slowly decaying, explicitly time-dependent, transport diffusivity of form $D(\Phi,t)=0.8t^{-0.20}\delta(\Phi)$ should lead to a universal curve when the moisture profiles are plotted as a function of $\xi=x/t^{0.40}$, as observed experimentally. Furthermore, an effective transport diffusivity $\delta(\Phi)$ $(\mathrm{cm}^2/\mathrm{s}^{0.80})$, which is fractional in the time variable, can then be obtained from the universal curve $\Phi(\xi)$ by employing Eq. (2), with $\eta$ replaced by $\xi$.

Figure 4 shows a plot of calculated values $\delta(\Phi)$ as a function of $\Phi=W/W_0$, where $W_0$ denotes water concentration in

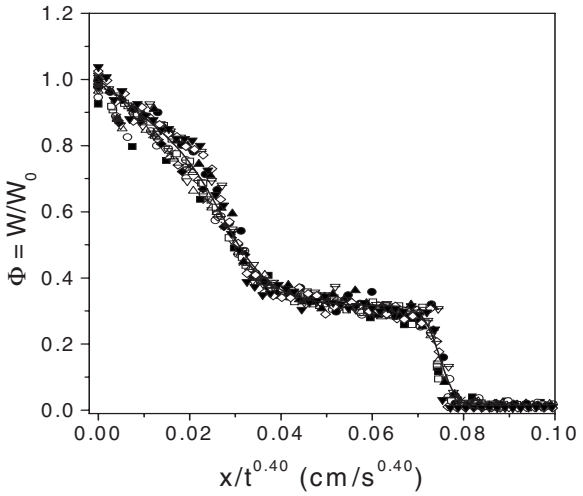


FIG. 3. Universal curve obtained from the profiles of Fig. 1 by plotting as a function of $x/t^{0.40}$. The solid line represents an empirical fitting function described in the text. Symbols denoting different times are the same used in Fig. 1.

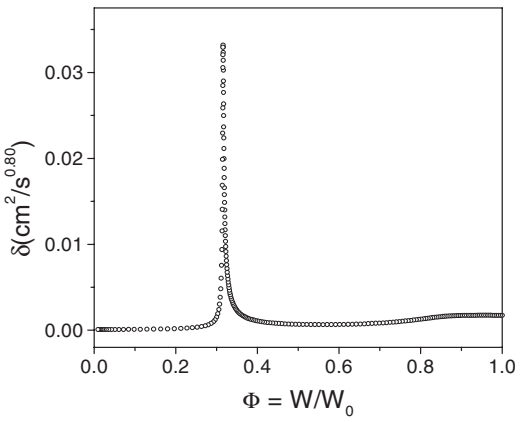


FIG. 4. Moisture dependence of the effective transport diffusivity $\delta(\Phi)$ obtained from the universal curve of Fig. 3 by assuming an explicit, separable, time-dependent permeability.

the fully saturated regime. In order to perform the operations involved in Eq. (2), the universal curve $W(\xi)/W_0$ was first represented by an analytical function [11,12] containing parameters, which were adjusted for a best fit of the data within the experimental uncertainty. The fitting function employed, which is plotted in Fig. 3 together with the collapsed data, was of the following form: $\Phi(\xi)=W(\xi)/W_0=0.686W_1(\xi)+0.369W_2(\xi)$ with $W_1(\xi)=[1-\mathrm{erf}(14.697\xi)][1+(32.15\xi)^6]^{-1}$ and $W_2(\xi)=0.85[1+(13.361\xi)^{40}]^{-1}$.

The moisture dependence of $\delta(\Phi)$ shown in Fig. 3 displays some features, which have not been observed in other porous systems and appear to vividly correlate with the pore morphology in paper. Instead of a monotonic, sometimes exponential [6,9], increase of the transport diffusivity with moisture content one observes a broad maximum near saturation $(\Phi=W/W_0\approx 1)$ and a narrow peak for $\Phi=W/W_0=0.31$, where the effective transport diffusivity is substantially larger. This peak corresponds to the fast moving precursor front.

In several cases where non-Fickian behavior is present it has been found experimentally that, for a considerable range of time, moisture profiles for imbibition can be collapsed into a universal curve when plotted as a function of $x/t^{\alpha/2}$ with $\alpha<1$, although we have found evidence, in some cases, that such a behavior may break down for very long times [18]. As shown above, this type of subdiffusive behavior, evident, for example, in Fig. 3, could be explained by assuming an explicit time dependence in the transport diffusivity of the following form: $\gamma(t)=\alpha t^{(\alpha-1)}$. However, it can also be derived, without any *a priori* assumption concerning a particular time dependence, by introducing the Riemann-Liouville fractional time derivative [19,20].

The use of derivatives of fractional order in the study of diffusion in porous media was introduced by Caputo [17] with the aim of accommodating memory effects, which could simulate a decrease of permeability with time in some types of flow. The Riemann-Liouville fractional derivative has been also employed in a generalized continuity equation, to study diffusion of carriers in the multiple-trapping regime [21]. For the imbibition problem, it has been shown [11] that a generalized continuity equation, where the time derivative

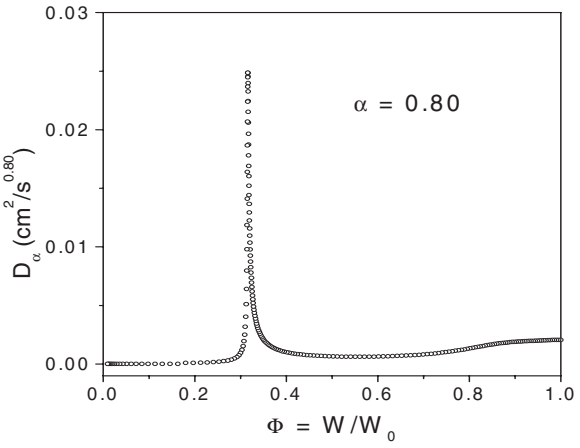


FIG. 5. Moisture dependence of the effective transport diffusivity $D_\alpha(\Phi)$ obtained from the universal curve of Fig. 3 by assuming a generalized continuity equation involving a Riemann-Liouville fractional time derivative with $\alpha=0.80$.

on the left-hand side of Eq. (1) is replaced by the Riemann-Liouville operator of order $\alpha$ $(0<\alpha<1)$ yields, for the boundary conditions prevailing in our imbibition experiment, a universal curve, provided the moisture profiles are plotted as a function of $\xi=x/t^{\alpha/2}$. Furthermore, the moisture dependence of the effective transport diffusivity $D_\alpha(\xi)$ can be obtained from the measured universal curve $\Phi(\xi)=W(\xi)/W_0$ by the following generalization [11] of Eq. (2):

$$D_\alpha(\xi)=\frac{d\xi}{d\Phi}\frac{1}{\Gamma(1-\alpha)}\int_\infty^\xi d\xi'\int_{\xi'}^\infty\left((2/\alpha)(1-\alpha)\frac{\Phi(\lambda)}{\lambda}-\frac{d\Phi(\lambda)}{d\lambda}\right)\frac{(\xi'/\lambda)^{2/\alpha}d\lambda}{[1-(\xi'/\lambda)^{2/\alpha}]^\alpha}. \quad (3)$$

Furthermore, $D_\alpha(\Phi)$ $(\mathrm{cm}^2/\mathrm{s}^\alpha)$ is obtained from $D_\alpha(\xi)$ by a numerical substitution using the universal curve $\Phi(\xi)$.

Figure 5 shows calculated values of $D_\alpha(\Phi)$ as a function of $\Phi=W/W_0$ obtained from Eq. (3) for $\alpha=0.80$ using the same fitting function as in Fig. 3. Since the results differ only slightly from those of Fig. 4 it appears that the same basic conclusions can be drawn, in the present system, independently of which model is employed for dealing with the departures from Fickian behavior. For small departures from Fickian behavior, such as for the value $\alpha=0.80$ obtained in the present case, this result is not surprising. In spite of quite different assumptions, both approaches are expected to yield identical results for $\alpha\to 1$. For much smaller values of $\alpha$ the differences would become more significant.

Although the choice of model to describe the small departure from Fickian behavior in the present case appears not to be critical, it is worth commenting about the applicability of each approach on more general grounds. The model leading to $\delta(\Phi)$ of Fig. 4 assumes that the permeability has a specific time dependence but is local in time and satisfies a continuity equation. On the other hand, in the fractional time derivative approach employed here the permeability is assumed to be time independent. However, given that the previous history makes a contribution to the value of the fractional derivative at the observation time, a memory effect is incorporated. The weight of the memory effect is larger, the smaller is $\alpha$ compared to unity. Moreover, the continuity equation is not strictly obeyed and $\Phi$ conservation in the fractional time diffusion equation [11] leading to Eq. (3), is only globally satisfied. This last aspect has led to the use of a fractional time derivative approach to describe systems where the diffusing species under study may convert into a different species, which can subsequently reconvert back. One such example is the diffusion of electrons in the conduction band of disordered systems that can be trapped in localized states and later released [21]. Another situation where a fractional time derivative approach could, in some cases, help in a parametrization of the problem is the transport of a fluid phase, which can transform into a vapor phase and subsequently recondense.

## IV. CONCLUSIONS

A coarse-grained approach based upon Darcy's law has been employed to characterize water imbibition in unsized paper cylinders molded under pressure. In this approach the details of the pore morphology are expected to be captured by a moisture-dependent transport diffusivity. Given the non-Fickian character of the imbibition process, two different approaches were employed to extract an effective transport diffusivity from measured moisture profiles. In both instances the practically coincident results were found to be quite different from what has been observed in other porous systems. Instead of a monotonic increase of the effective transport diffusivity with moisture content two peaks are observed. A broad maximum near saturation $(W/W_0\approx 1)$ and a narrow peak for $W/W_0\approx 0.31$, where the effective transport diffusivity is substantially larger. This peculiar behavior, which is consistent with the existence of a precursor front in paper fibers [14], suggests a correlation with microscopic observations obtained from cryo-SEM. Such measurements together with estimates based on fluid dynamics, point toward a transport mechanism dominated by film flow along channels formed by fiber overlap.

## ACKNOWLEDGMENTS

We wish to thank Professor R. E. de Souza for assistance. This work has been supported by Conselho Nacional de Desenvolvimento Científico e Tecnológico CNPQ (Brazilian agency) and by the Research Council of Norway.

[1] E. W. Washburn, Phys. Rev. **17**, 273 (1921).
[2] J. Bico and D. Quéré, Europhys. Lett. **61**, 348 (2003).
[3] R. J. Roberts, T. J. Senden, M. A. Knackstedt, and M. B. Lyne, J. Pulp Pap. Sci. **29**, 123 (2003).
[4] R. J. Gummerson, C. Hall, W. D. Hoff, R. Hawkes, G. N. Holland, and W. S. Moore, Nature (London) **281**, 56 (1979).
[5] C. Hall, Cem. Concr. Res. **37**, 378 (2007).
[6] S. Blackband and P. Mansfield, J. Phys. C **19**, L49 (1986).
[7] L. Pel, Ph.D. thesis, Technische Universiteit, 1995.
[8] L. Pel, K. Kopinga, G. Bartram, and G. Lang, J. Phys. D: Appl. Phys. **28**, 675 (1995).
[9] D. A. Lockington and J.-Y. Parlange, J. Phys. D: Appl. Phys. **36**, 760 (2003).
[10] H. L. Frandsen, L. Damkilde, and S. Svensson, Holzforschung **61**, 563 (2007).
[11] E. N. de Azevedo, P. L. de Sousa, R. E. de Souza, M. Engelsberg, Mirla de N. do N. Miranda, and M. A. Silva, Phys. Rev. E **73**, 011204 (2006).
[12] E. N. de Azevedo, D. V. da Silva, R. E. de Souza, and M. Engelsberg, Phys. Rev. E **74**, 041108 (2006).
[13] E. Mark Haacke, Robert W. Brown, Michael R. Thompson, and Ramesh Venkatesan, *Magnetic Resonance Imaging-Physical Principles and Design* (Wiley, New York, 1999).
[14] A. S. Balankin, R. G. Paredes, O. Susarrey, D. Morales, and F. C. Vacio, Phys. Rev. Lett. **96**, 056101 (2006).
[15] R. Lucas, Kolloid-Z. **23**, 15 (1918).
[16] J. Crank, *The Mathematics of Diffusion* (Oxford University Press, London, 1975).
[17] M. Caputo, Geothermics **28**, 113 (1999).
[18] Lars Ramstad Alme, thesis, Norwegian University of Science and Technology, M.S., 2007.
[19] E. Barkai, R. Metzler, and J. Klafter, Phys. Rev. E **61**, 132 (2000).
[20] R. Metzler and J. Klafter, Phys. Rep. **339**, 1 (2000).
[21] J. Bisquert, Phys. Rev. Lett. **91**, 010602 (2003).